

A tunable colloidal quantum dot photo field-effect transistor

Subir Ghosh, Sjoerd Hoogland, Vlad Sukhovatkin, Larissa Levina, and Edward H. Sargent^{a)}
*Department of Electrical and Computer Engineering, University of Toronto, 10 King's College Road,
 Toronto, Ontario M5S 3G4, Canada*

(Received 13 July 2011; accepted 22 August 2011; published online 6 September 2011)

We fabricate and investigate field-effect transistors in which a light-absorbing photogate modulates the flow of current along the channel. The photogate consists of colloidal quantum dots that efficiently transfer photoelectrons to the channel across a charge-separating (type-II) heterointerface, producing a primary and sustained secondary flow that is terminated via electron back-recombination across the interface. We explore colloidal quantum dot sizes corresponding to bandgaps ranging from 730 to 1475 nm and also investigate various stoichiometries of aluminum-doped ZnO (AZO) channel materials. We investigate the role of trap state energies in both the colloidal quantum dot energy film and the AZO channel. © 2011 American Institute of Physics. [doi:10.1063/1.3636438]

Most photodetectors function either as photodiodes or as photoconductors: photodiodes offer fast response and low dark current, while photoconductors provide built-in gain associated with the use of long-lived sensitizing centers. The concept of a phototransistor, such as a photo-field-effect-transistor (photoFET),¹ offers an attractive possibility: gain united with a lowered dark current compared to the photoconductor, achieved if the thickness of the current-carrying channel can be chosen independently from the thickness of the light-absorbing layer.

Here, we report a versatile photoFET that benefits from a broad spectrum of detection, spanning the visible and portions of the short-wavelength infrared spectral region. We present two of the four ingredients necessary to the realization of a highly sensitive photodetector based on the photoFET concept: we successfully transfer photoelectrons from the sensitizing material to the electron-accepting channel (EAC), and we obtain photocurrents through the recirculation of secondary injected photocarriers flowing along the channel. Further work will be required to realize a sensitizing layer having sufficiently high electron mobility that a fully light-absorbing thickness of this medium can efficiently inject all carriers into the channel; and to deposit an ultrathin channel compatible with low dark current.

Our device uses colloidal quantum dots (CQDs) as the sensitizing material to form the photo gate. CQDs offer tunability of the bandgap, and thus the spectral range of light sensing in a photodetector, through the size of the nanoparticles. Since CQDs are solution processable, they are compatible with low-cost, large-area processes.

We utilize a sub-monolayer film of PbS CQD of a variety of sizes as the sensitizing material. Aluminum-doped zinc oxide (AZO) serves as the electron-accepting channel. We employ no conductivity-enhancing treatments to the CQD films—instead of employing crosslinking treatments using short dithiols,² we leave the quantum dots capped with oleic acid. This, combined with our use of a submonolayer of CQDs, ensures that our study focuses on electron injection

into the channel, followed by conduction within the channel, since the photogate material has negligible conductance compared to the channel.

As schematically drawn in Figure 1, the photoFET comprised of an EAC atop a glass substrate with pre-patterned gold electrodes, with spacings ranging from 2.5 μm to 100 μm and 3 mm length. This EAC consisted of an AZO film of 50 nm thickness, deposited through RF sputtering directly onto the patterned glass substrate. PbS CQDs of ultra-low concentration (0.5 mg/mL), dispersed in octane, were spin-cast onto the AZO covered substrate and then removed on and near the contact pads to ensure that the film is confined to the active region of the device. An electric field was applied across the source

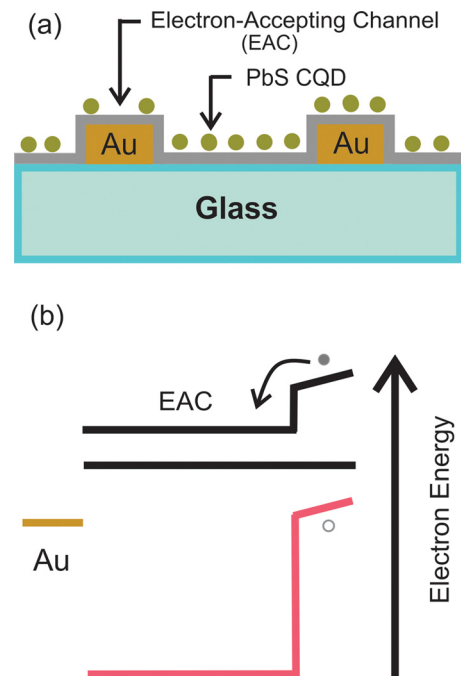


FIG. 1. (Color online) (a) Schematic of the device structure used in this study. (b) Energy band diagram showing dissociation of electrons upon photo-excitation at the oxide semiconductor and the colloidal quantum dot interface. Photo-excited electrons are subsequently collected through the Au electrode by applying an electric field.

^{a)} Author to whom correspondence should be addressed. Electronic mail: ted.sargent@utoronto.ca.

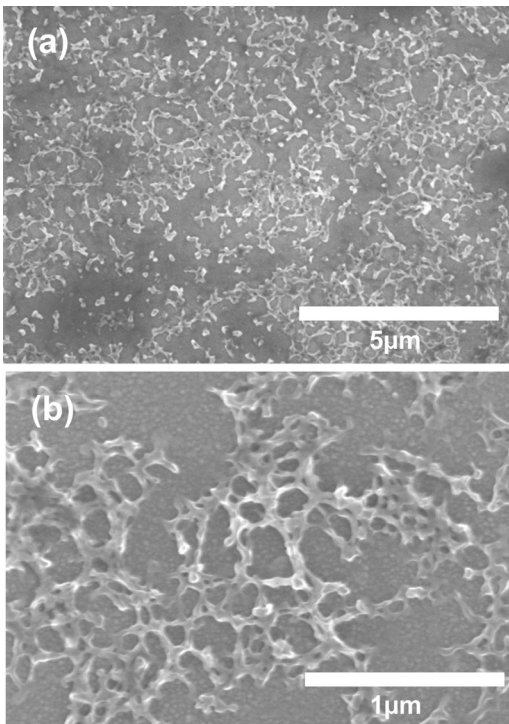


FIG. 2. SEM images of a colloidal quantum dot film atop AZO at magnification (a) 10 K and (b) 50 K. The CQD film was deposited by spin-coating of PbS CQDs dispersed in octane, at a concentration of 0.5 mg/mL. The images clearly show that these conditions yield the desired discontinuous CQD films.

and the drain electrodes to collect photocharges transferred to the channel upon photoexcitation.

The AZO channel was deposited using an RF sputtering system (Angstrom Engineering) under oxygen partial pressures ($[O_2]:[O_2 + Ar]$) of 5%, 10%, and 20%. Introduction of oxygen increases the resistivity of the film and also changes the electron affinity of the AZO material. The electron affinity of 5%, 10%, and 20% oxygen-rich AZO films was measured with cyclic voltammetry,³ yielding -4.2 eV, -4.34 eV, and -4.39 eV compared to the vacuum level, respectively. This trend is consistent with published findings that the electron affinity of AZO films becomes deeper as the oxygen content is increased during deposition.⁴

We confirmed with SEM that the CQD film was discontinuous (Figure 2), thus ensuring that the only lateral conduction path was via the channel. We further confirmed this by spin-coating CQDs under identical conditions onto pre-patterned substrates, without the AZO present. No measurable dark or light current was observed from these controls.

Figure 3(a) shows absorption spectra of different CQD batches synthesized to yield different sizes and corresponding bandgaps of 730 nm, 854 nm, 950 nm, and 1475 nm. The Figure 3(b) shows the relative band position of the dots with respect to the different AZO channel materials used in this study. Bandgap and the electron affinity of the CQDs were estimated based on the work of Hyun *et al.*⁵ With decreasing bandgap, the conduction bandedge of the CQDs comes closer to the conduction bandedge of the AZO, thus potentially decreasing the injection efficiency of photo-electrons into the channel.

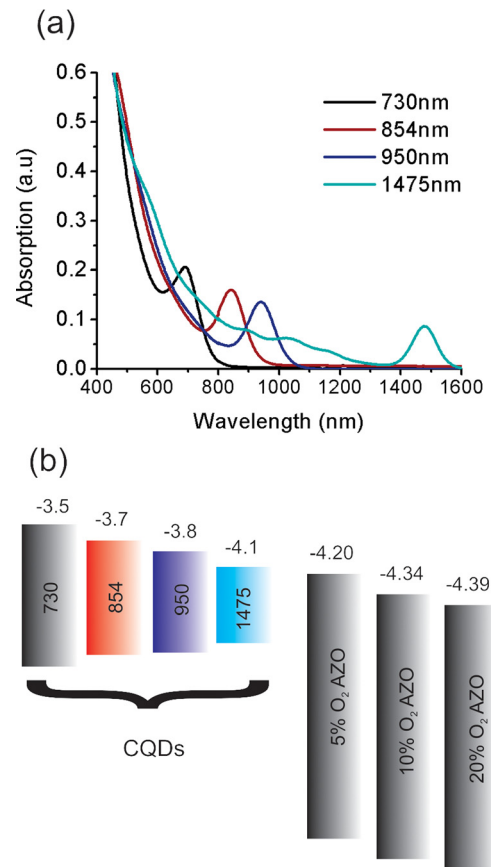


FIG. 3. (Color online) (a) Absorption spectra of different CQDs used in this study (b) Band alignment of AZO films with respect to colloidal quantum dots. The electron affinity of AZO films was calculated from cyclic voltammetry measurements whereas the electron affinity of colloidal quantum dots was estimated based on the work of Hyun *et al.*⁵

All devices were fabricated under identical conditions for each CQD size—AZO channel material combination. Each sample was subsequently subjected to 627 nm light modulated at a frequency of 0.2 Hz. Figures 3(a)–3(d) show the representative time traces of the photoresponse for the large and small bandgap dots on AZO channels, deposited under low and high oxygen conditions. Figures 3(e) and 3(f) depicts the calculated external gain for the 4 dot sizes and 3 different AZO channels under different illumination intensities. It is found that the photoconductive gain increases with CQD size. In part, we attribute the increased gain to the higher absorption of sub-monolayer of the larger quantum dots⁶ at the red excitation wavelength. Of principal note, though, is the fact that efficient photoelectron transfer is achieved into AZO for all choices of CQD size in this study.

Increase of the oxygen partial pressure during the deposition of the AZO channel material not only increases the electron affinity but also has the effect of decreasing the conductivity of the AZO film as a result of decreasing oxygen vacancies in the AZO film. These oxygen vacancies may serve as traps in our devices causing carriers to recombine and, therefore, a decrease in the gain of the photoFET. Indeed, the external gain was found to decrease as the oxygen partial pressure is increased. In addition, as a result of the reduced trap density with increased oxygen partial pressure, temporal response as well as dark current of our devices significantly improved—a substantial fast-response

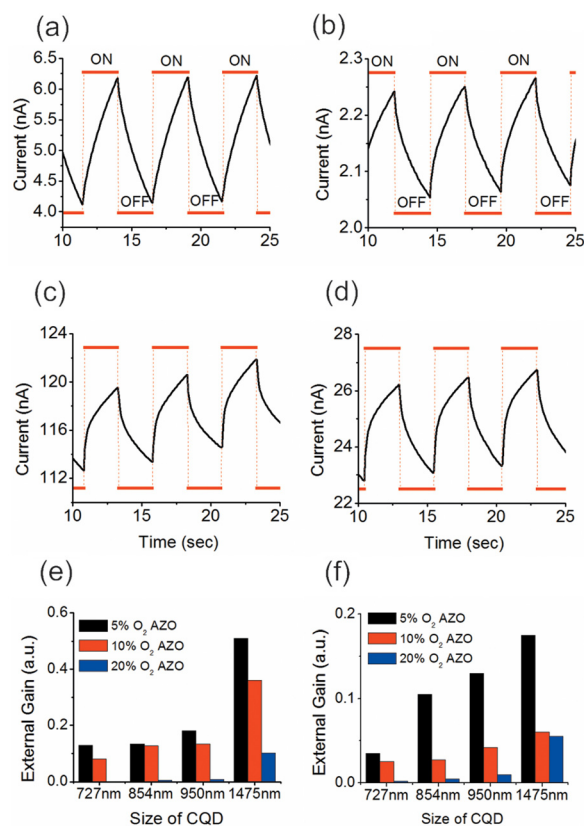


FIG. 4. (Color online) Time-dependent photoresponse (indicated by ON-OFF sequence) of sub-monolayer films of colloidal quantum dots with bandgaps of (a) and (b) 727 nm and (c) and (d) 1475 nm, on top of (a) and (c) 5% and (b) and (d) 20% O₂ rich AZO channels. Measurements were carried out under an applied field of 1000 V/cm and illumination of red light (time period 5 s) of intensity 225 μW/cm². Calculated external photoconductive gains at illumination intensities of (e) 12 μW/cm² and (f) 645 μW/cm², showing that the gain increases as the band offset between the EAC material and the CQDs decreases. The photoconductive gain also decreases with light intensity.

component coincident with reduced dark current appears in the photocurrent response signal as the oxygen content of the AZO is changed from 5% to 20% (Figures 4(a)–4(d)). The temporal response, for a certain electrode material, can also be significantly manipulated through proper selection of the size of CQDs, as is evident in Figures 4(a) and 4(c). These findings indicate the ability to optimize the photoFET properties through the joint selection of nanocrystals and electron accepting channel.

The illumination intensity dependent studies show that the photoconductive gain decreases with light intensity for all CQD sizes and AZO materials used in this study (Figs. 4(e) and 4(f)). This effect may be attributed to bimolecular recombination⁷ or filling up of the lowest lying longest lived trap states at high intensities,⁸ which, in effect, decreases the external gain at higher intensity of illumination.

We compared these results with sputtered TiO₂, an electrode successfully employed in colloidal quantum dot solar cells. Cyclic voltammetry confirmed that TiO₂ has a similar bandedge position to the AZO used herein. Devices employing TiO₂ showed sharper temporal response, similar to the

fast response component of Figure 4(d), and at least, one order of magnitude lower photoconductive gain than in the case of AZO. This change in properties may be attributed to the lower density of oxygen vacancies in the TiO₂ channel material.

The results presented herein indicate that photoelectron transfer is achieved for any of the sizes of dots considered herein (730 nm bandgap to 1475 nm bandgap) to any of the AZO electrodes considered herein (−4.2 eV conduction band edge to −4.4 eV conduction bandedge). The findings suggest that AZO could in principle serve as a particularly appropriate electrode in PbS colloidal quantum dot photovoltaics seeking long-wavelength operation, such as the smallest-bandgap junction of a triple-junction solar cell (~1600 nm bandgap desired).

The higher response seen from the shallower-electron-affinity electrode compared to the deeper-electron-affinity electrode is not explainable by the band offsets. Instead, we propose that the oxygen concentration during sputter deposition can appreciably modify both electron mobility and trap states within the AZO. The dramatically higher response obtained using the smaller-bandgap quantum dots is not fully explained via higher absorption alone: combined with differences in temporal response depending on quantum dot size, these results suggest that the energy levels of the trap states at the channel-dot interface are a joint property of the quantum dots and the channel material band and trap energy levels.

In summary, this work reports the realization of a photo-transistor in which light absorption and photocarrier conduction are separated into distinct materials. Communication among the sensitizer and the channel occurs via electron transfer associated with the heterointerface. The trap state energies and densities in the channel appear to play a significant role in the amplitude of photoresponse and in the temporal response, of the resulting device.

This publication is based in part on work supported by an award (No. KUS-11-009-21) made by King Abdullah University of Science and Technology (KAUST), by the Ontario Research Fund Research Excellent Program, by the Natural Sciences and Engineering Research Council (NSERC) of Canada, Angstrom Engineering and Innovative Technology. We acknowledge the assistance of Dr. Ratan Debnath and Dr. Xihua Wang.

¹T. P. Osedach, S. M. Geyer, J. C. Ho, A. C. Arango, M. G. Bawendi, and V. Bulovic, *Appl. Phys. Lett.* **94**(4), 043307 (2009).

²E. J. D. Klem, H. Shukla, S. Hinds, D. D. MacNeil, L. Levina, and E. H. Sargent, *Appl. Phys. Lett.* **92**(21), 212105 (2008).

³E. Kucur, J. Riegler, G. A. Urban, and T. Nann, *J. Chem. Phys.* **119**(4), 2333 (2003).

⁴S. Brehme, F. Fenske, W. Fuhs, E. Nebauer, M. Poschenrieder, B. Selle, and I. Sieber, *Thin Solid Films* **342**(1–2), 167 (1999).

⁵B. R. Hyun, Y. W. Zhong, A. C. Bartnik, L. F. Sun, H. D. Abruna, F. W. Wise, J. D. Goodreau, J. R. Matthews, T. M. Leslie, and N. F. Borrelli, *ACS Nano* **2**(11), 2206 (2008).

⁶C. A. Leatherdale, W. K. Woo, F. V. Mikulec, and M. G. Bawendi, *J. Phys. Chem. B* **106**(31), 7619 (2002).

⁷R. R. Mehta and B. S. Sharma, *J. Appl. Phys.* **44**(1), 325 (1973).

⁸G. Konstantatos and E. H. Sargent, *Nat. Nanotechnol.* **5**(6), 391 (2010).